

## Broadband and long lifetime plasma-antenna in air initiated by laser-guided discharge

Francis Théberge,<sup>1,a)</sup> Jean-François Gravel,<sup>1</sup> Jean-Claude Kieffer,<sup>2</sup> François Vidal,<sup>2</sup> and Marc Châteauneuf<sup>1</sup>

<sup>1</sup>Defence R&D Canada Valcartier, 2459 de la Bravoure Blvd., Québec, Québec G3J 1X5, Canada

<sup>2</sup>INRS-EMT, 1650 Lionel-Boulet Blvd., Varennes, Québec J3X 1S2, Canada

(Received 24 May 2017; accepted 23 July 2017; published online 14 August 2017)

In this work, we demonstrate the coupling and emission of radio-frequency (RF) signals from laser-guided discharge in ambient air. The produced 100-cm long plasma-antenna is broadband and can emit RF signals for more than 2 ms, which corresponds to an enhancement of the plasma-antenna lifetime of 4 orders of magnitude relative to previous demonstrations using laser-based plasma filamentation. The generation of large diameter plasma-antennas in the air allows to broadcast RF signals efficiently from  $\sim 10$  MHz to few tens of GHz. [<http://dx.doi.org/10.1063/1.4985045>]

Plasma-antenna technologies are becoming more ruggedized<sup>1</sup> and usually employ ionized gas enclosed in a tube as the conducting element of a transceiver.<sup>2–5</sup> These plasma-antennas present numerous benefits in wireless communications and defence applications that standard metallic antennas cannot achieve.<sup>3–5</sup> For example, plasma-antennas can greatly reduce co-site interference by synchronizing/activating on-demand adjacent plasma-antennas, which is important for many forms of digital communications and radar types.<sup>2,5</sup> Another fundamental distinguishing feature is that after sending a short pulse, the plasma-antenna can be de-ionized, eliminating the ringing associated with traditional metal antennas. For defence applications, and in addition to their broadband and high-speed communication capabilities, plasma-antennas present stealth features by being quickly de-ionized when scanned by other radars.<sup>5</sup> These concepts have been widely demonstrated with low density plasma generated inside dielectric tubes. The physical confinement of such plasma-antennas limits the speed at which they can be re-oriented and configured. To solve these challenges, plasma-antennas produced with laser beams ionizing the air were suggested.<sup>6–10</sup>

The lifetime of long and high-density plasma channels is a critical parameter for plasma-antennas, since it limits the maximum duration for the guiding and emission of microwaves. Demonstrations of microwave guiding using laser-produced plasma filaments in air have been widely confirmed.<sup>6–10</sup> The initial laser-produced plasma filaments, used for these results, are generated in air when the laser peak power exceeds a threshold named the critical power for self-focusing.<sup>11</sup> During their propagation in air, these ultrashort and intense laser pulses self-focus on themselves up to laser intensity sufficiently high to ionize the air. Starting from this zone, an automatic dynamic equilibrium occurs mainly between the laser self-focusing, plasma generation, plasma defocusing, and laser diffraction, which creates thin and long plasma channels left behind the laser path.<sup>12–14</sup> However, the limited lifetime of the plasma column produced by laser filaments restricted the microwave guiding duration to a few nanoseconds, constraining considerably the communication

capability of such plasma-antennas. Previous works succeeded in increasing the laser-produced plasma lifetime by using an external electric field,<sup>15,16</sup> and such a combination allowed the increase of the plasma-antenna lifetime in air up to 100 ns.<sup>17</sup> Recent work reported an increase in the laser-guided plasma lifetime up to 2 ms in air by using a hybrid high-voltage source.<sup>18</sup> By using this method, we demonstrate in this paper the possibility to produce broadband plasma-antennas in air having a lifetime of 4 orders of magnitude longer than previous laser-based demonstrations.

The plasma-antenna produced in our experiments is initiated by the laser-guiding of AC-discharge,<sup>18</sup> generating a conductive and low density air linear channel having a length of 100 cm. Following the ignition of this laser-guided AC discharge, a subsequent DC glow discharge enhances the electron density and the diameter of the plasma column through the Joule effect. The hybrid high-voltage source used in our experiments and the methodology to produce large diameter and long plasma channels with high conductivity in air are described in Ref. 18. Briefly, it consists of solid-state Tesla coil (AC high-voltage source) combined in series with a high load 30 kV capacitance (DC high-voltage source), allowing us to store a 500-J electric energy. Ultrashort laser pulses of 0.15 J, from a portable chirped pulse amplification Ti:Sapphire system,<sup>19</sup> were focused using a 3-m focal length lens to produce a bundle of plasma filaments in air having a total length of 1.5 m. The conductive laser filaments were generated 1 cm above the electrodes distanced by a 100-cm air gap [see Fig. 1(a)]. The filament bundle was positioned so that it started slightly before the high-voltage electrode. The highest plasma density filaments produced by the laser around the lens focus were positioned at the center of the radio-frequency (RF) coupler and passed above the grounded electrode. The RF coupler used to inject the RF signal into the plasma column is shown in Fig. 1(b). The RF coupler is made of 5 turns spaced by 5 mm and coiled around a 35-mm outside diameter tubular insulator (inner diameter of 15 mm) having a relative permittivity of 3. The RF coupler is encapsulated in a cylindrical Faraday cage to minimize the RF leakage in the absence of the plasma-antenna. The synchronization between the laser pulse and the hybrid high-voltage source was optimized for the

<sup>a)</sup>francis.theberge@drdc-rddc.gc.ca

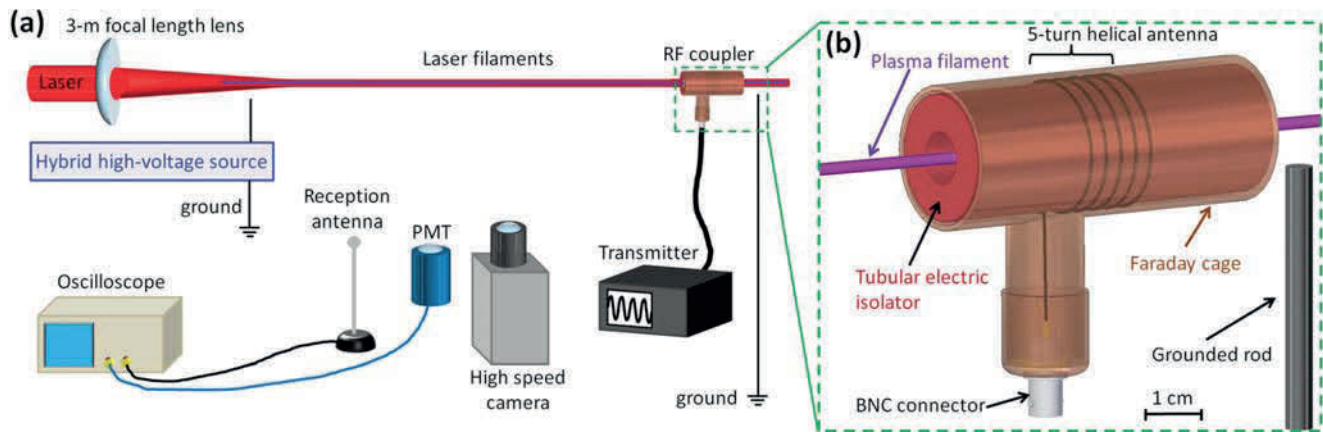


FIG. 1. (a) The schematic of the experimental setup for monitoring the plasma-antenna produced by laser-guiding of hybrid high-voltage discharges. (b) Schematic representation of the plasma-antenna traversing the RF coupler.

maximum laser-guided length ( $>95\%$ ) over the 100-cm air gap [see Fig. 2(a) for a side-picture of the laser-guided plasma channel]. During all measurements, the laser filaments and the surrounding laser energy reservoir<sup>20,21</sup> did not impact the electrodes. Temporally resolved images of laser-guided discharges were captured using a high-speed camera with time resolution down to few microseconds per frame. Concurrently, a photomultiplier tube (PMT) with a large field of view and a 1 ns resolution was used to monitor the

light emission over the whole length of the plasma column. Finally, a standard 25 W transmitter (Motorola Maxar 80) used as the RF source around 173 MHz was connected to the RF coupler. A typical 40.6-cm long metallic antenna used as the reception antenna was positioned at 4 m from the plasma column. The RF signal emitted by the plasma-antenna was collected by the reception antenna and directly recorded with a 2 GHz oscilloscope without using a RF amplifier or filter.

Figure 2(b) presents the temporal evolution of the plasma fluorescence strength, which stands for more than 2 ms and is nearly proportional to the square of the current flowing in the plasma channel.<sup>22</sup> The short fluorescence peak around time zero in Fig. 2(b) corresponds to the fluorescence emitted by the initial laser-guided leader and the discharge of the AC high-voltage source.<sup>18</sup> The time zero corresponds to when the laser pulse passes between the electrodes and generates a bundle of plasma filaments. Following the AC discharge, the AC electric field vanishes after few tens of microseconds, but a conductive and low air density channel remains along the laser path and this will allow the subsequent 500-J DC discharge from the high load capacitance.<sup>18</sup> The high impedance of this discharging circuit takes some time to build up the high-current, making the fluorescence to peak 350  $\mu$ s after the laser pulse. This peak of fluorescence corresponds to a peak current of  $\sim 100$  A, and the resulting Joule heating induces a hydrodynamic expansion transverse to the channel axis. The plasma column diameter quickly increased from  $\sim 100$   $\mu$ m to 4 mm (full width at  $1/e^2$ ) at the peak current. Afterward, the current decreased but the Joule heating was sufficient to increase the plasma column diameter up to 7 mm at the end of the DC discharge.

Figure 2(c) presents two samples of the RF signal recorded from the distant reception antenna when the transmitter connected to the RF coupler was turned-off. The electromagnetic (EM) noise pulse observed around the time-zero is produced by the abrupt laser-guided AC discharge. This electromagnetic noise pulse ceases few tens of microseconds after the AC discharge, and no electromagnetic noise was detected afterward during the DC discharge. The absence of electromagnetic noise following the AC discharge indicates that the produced air channel was very conductive and eliminated the possibility of sparking during the DC glow discharge.

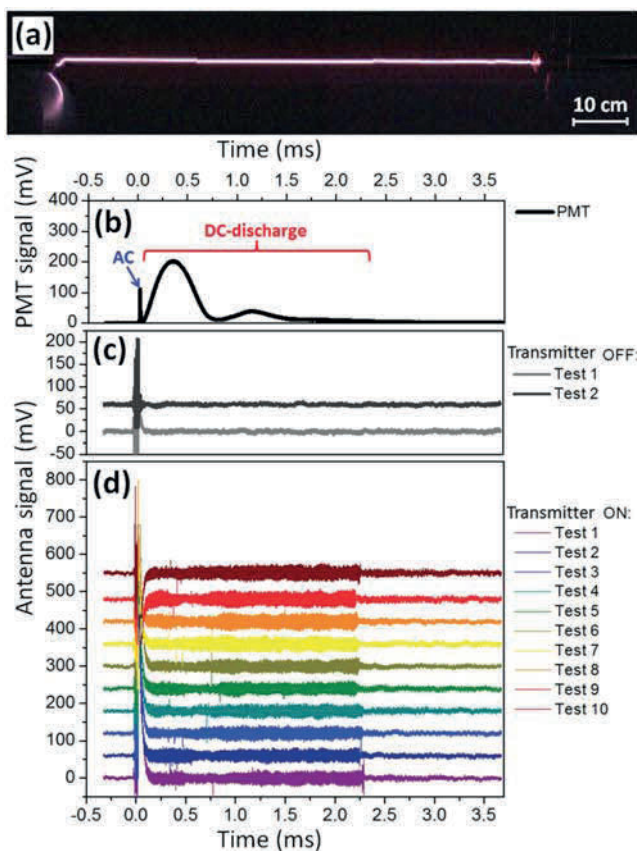


FIG. 2. (a) Color image taken by a high-speed camera of the laser-guided discharge over the 100-cm air gap. (b) Plasma fluorescence strength detected by a photomultiplier tube (PMT). (c) Temporal waveform of the RF signal detected with the distant reception antenna without activating the transmitter and (d) by activating the transmitter (Note: RF signals are vertically shifted for clarity).

Figure 2(d) presents ten samples of RF signals recorded from the distant reception antenna when the transmitter was continuously producing a carrier at 173.13 MHz. During the generation of the plasma-antenna, we still observe around time-zero the electromagnetic noise pulse induced by the laser-guided AC-discharge and the transient polarity depends on the AC-voltage polarity at the connection of the laser-guided leader between both electrodes. After the transient, a quasi-constant RF signal at 173.13 MHz was measured and persisted up to a time of  $\sim 2.25$  ms, corresponding to the end of the DC glow discharge.

Figure 3(a) presents the RF signal emitted by the 100-cm long plasma-antenna before and during the laser-guided discharge. Narrow temporal windows of the signal detected are sampled and expanded in Figs. 3(b)–3(e) for the timings of  $-200 \mu\text{s}$ ,  $100 \mu\text{s}$ ,  $1$  ms, and  $2$  ms, respectively. The corresponding power spectra of the sampled regions are presented in Fig. 3(f). For reference and comparison, the power spectrum of the signal emitted when the plasma column is replaced by a 100-cm long metallic rod of 5-mm diameter (black line with grey fill) is also shown in Fig. 3(f). It is interesting to note that the RF power emitted at 173.13 MHz by the plasma-antenna was only 6 dB lower than for the metallic rod.<sup>17</sup> The power of the RF signal emitted by the plasma-antenna is more than 50 times higher than the leak of the RF coupler [green line filled with grid in Fig. 3(f)]. The distribution of the RF power spectrum emitted by the plasma-antenna is very similar to the RF signal injected into the RF coupler, pointing out the large bandwidth emissivity of the plasma-antenna. The four RF channels (172.41 MHz–173.34 MHz) from the transceiver were tested with this plasma-antenna, and their emitted RF powers were very similar for each channel.

The fluorescence signal of the plasma-antenna shown in Fig. 2(b) indicates that the current flowing in the plasma column oscillates due to ringing of the inductance and capacitance of the discharge circuit. Nevertheless, the conductivity of the plasma column remained around 1000 S/m during the whole discharge.<sup>18,23</sup> Since the RF power emitted by the plasma-antenna was only 6 dB lower than for the metallic rod having a conductivity of 1 MS/m ( $\sim 1000$  times higher than the plasma-antenna), the coupling of the RF signal into the plasma column is weakly dependent on its conductivity

or its plasma density. The coupling of the RF signal to the plasma column occurs through the induction of EM wave propagating at the interface between the plasma column and the surrounding air.<sup>8,10,24,25</sup> The surface wave theory indicates that such plasma-antennas are broadband and confirms that the attenuation at the surface of the plasma column is weakly dependent from the plasma density as shown in simulations presented in Figs. 4(a) and 4(b). In Fig. 4(a), for a fixed 4-mm diameter plasma-antenna, the simulated RF frequency ( $\nu_{\text{rf}}$ ) of the surface wave at which the attenuation is minimal is inversely proportional to the plasma frequency ( $\omega_p$ ) in the limit where  $\nu_{\text{rf}} \ll \omega_p$ . In Fig. 4(b), it is observed that by changing the plasma density by two orders of magnitude in the simulations, the surface wave attenuation changes by less than a factor of three for the 173 MHz frequency used in our experimentation. However, the attenuation of the surface wave coupled on the plasma column is very dependent on the plasma column diameter, as shown in Fig. 4(b). This is mainly due to the fact that a larger plasma column can sustain more easily the surface mode for long RF wavelengths. For a RF signal of 173 MHz, the attenuation ( $\alpha$ ) decreases by two orders of magnitude when the plasma column diameter increases from 0.5 mm to 4 mm, for both plasma densities of  $5 \times 10^{16}$  and  $5 \times 10^{18} \text{ cm}^{-3}$ . For a plasma column diameter larger than 1.5 mm, the attenuation length corresponding to  $1/\alpha$  is longer than the 100-cm long plasma-antenna, indicating that the surface wave is radiated over its whole length at 173 MHz. For a smaller plasma-antenna diameter, the attenuation length is shorter than the laser-guided discharge and only a portion of the plasma column acts as an antenna, therefore lowering the emission of the RF signal.

Since the plasma column diameter is an important factor influencing the surface wave attenuation, the measured plasma-antenna diameter produced by the laser-guided discharge is shown as a function of time (logarithmic scale) in Fig. 4(c). The plasma column diameter increases very rapidly after its ignition by the laser filaments and reaches a diameter larger than 1.5 mm after  $100 \mu\text{s}$ . Based on the simulated surface-wave attenuation and the measured plasma column diameter, shown in Figs. 4(b) and 4(c), respectively, the attenuation of the plasma-antenna could be estimated as a function of time, and the result is shown in Fig. 4(d).

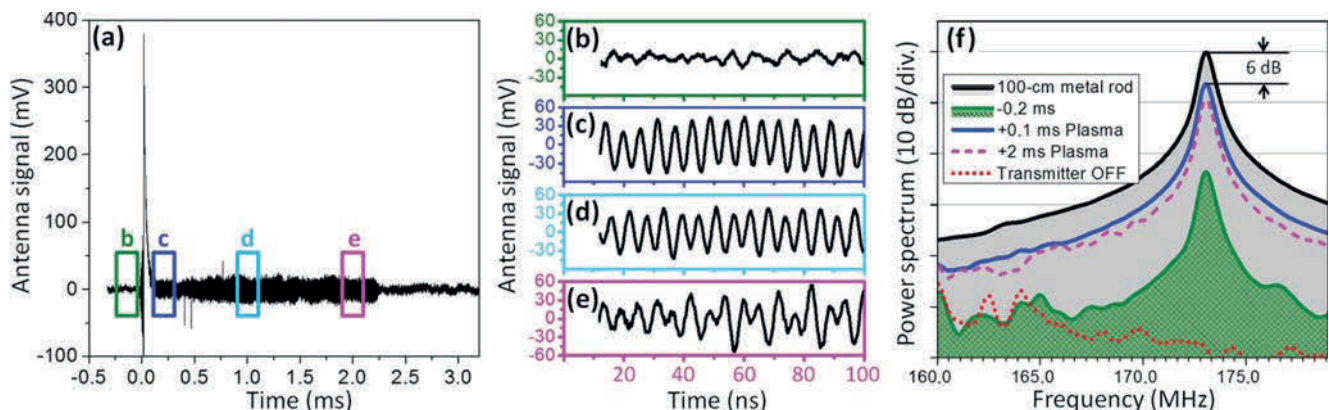


FIG. 3. (a) Temporal waveform of the RF signal emitted by the plasma-antenna and detected with the 40.6-cm long metallic antenna. (b) Zoomed RF signal sampled  $200 \mu\text{s}$  before the laser-guided discharge, (c)  $100 \mu\text{s}$ , (d)  $1$  ms, and (e)  $2$  ms after the ignition of the plasma column. (f) Power spectrum of the sampled RF signals.



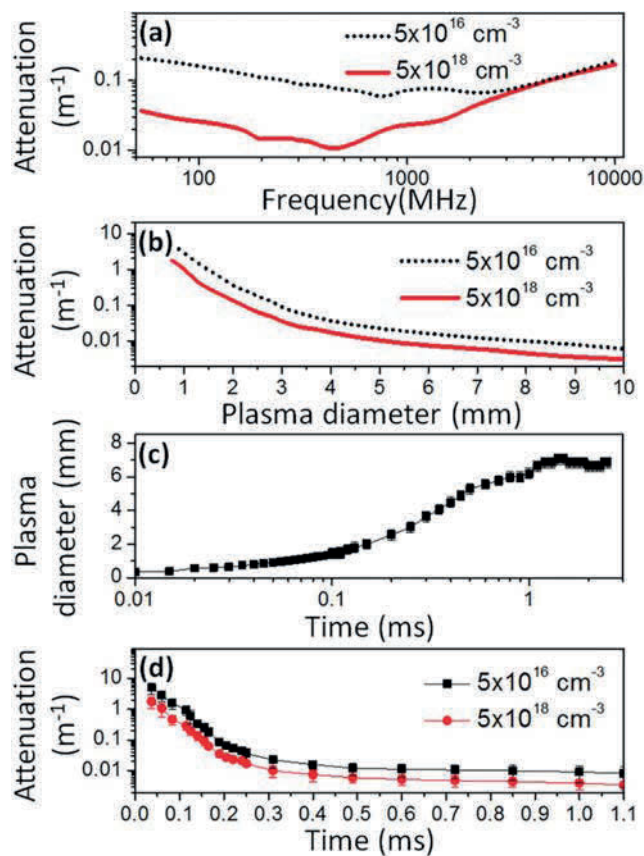


FIG. 4. (a) Simulated surface wave attenuation as a function of the RF frequency (plasma column diameter fixed at 4 mm) and (b) as a function of the plasma-antenna diameter (RF frequency fixed at 173 MHz). For both figures, the plasma densities of  $5 \times 10^{16} \text{ cm}^{-3}$  and  $5 \times 10^{18} \text{ cm}^{-3}$  were simulated. (c) Measured plasma channel diameter (full width at  $1/e^2$ ) as a function of time. (d) Calculated surface wave attenuation at 173 MHz as a function of time for the tested plasma-antenna by considering two different plasma densities.

Independently of the plasma density, the plasma-antenna attenuation is very low 100  $\mu\text{s}$  after its ignition by the laser filaments. The higher attenuation for time delays inferior to 100  $\mu\text{s}$  explains the lower amplitude of the 173 MHz signal detected at these timings, as observed, for example, in Fig. 3(a). Finally, it is important to note that without the high-voltage discharge, the initial plasma column produced by the laser filaments has an approximate diameter of 70  $\mu\text{m}$ , a peak plasma density around  $10^{16}$  electrons/ $\text{cm}^3$ , and a lifetime of few nanoseconds.<sup>26</sup> Such parameters can guide efficiently surface waves of frequencies higher than  $\sim 1$  GHz only during the limited lifetime of the plasma filaments. In order to make broadband laser-based plasma-antennas efficient from  $\sim 10$  MHz to a few tens of GHz, large diameter plasma columns must be produced by enhancing them with an external high-voltage source. Therefore, using the hybrid high-voltage source has the dual advantages of extending the plasma lifetime and broadening the spectral range of plasma-antennas.

In conclusion, the highly conductive plasma-antenna produced in ambient air by the laser-guiding high-voltage discharge method allowed to transmit efficiently a RF carrier of 173 MHz. The produced plasma column functioned as a transmitter for more than 2 ms, which is a 4 order increase

compared to previous demonstrations based on laser filamentation. Due to the high current flowing in the laser-guided discharge, the plasma column diameter quickly increased up to a few millimeters in diameter, allowing to transmit efficiently the RF signal over a broad frequency range. Interestingly, we demonstrated through simulations that the attenuation of the surface wave on the plasma-antenna is weakly dependent on plasma density, but very dependent on the plasma column diameter. Finally, we note that a possible improvement to the current setup would consist in commencing the laser-guiding of the discharge with an initial large diameter plasma column produced by the filamentation of far-infrared ultrashort laser pulses.<sup>27–29</sup>

This work was supported by a Defence Research & Development Canada Program. The authors acknowledge technical support from Gaston Nadeau and Pascal Duchesne.

- <sup>1</sup>J. Zhao, S. Wang, H. Wu, Y. Liu, Y. Chang, and X. Chen, *Appl. Phys. Lett.* **110**, 094108 (2017).
- <sup>2</sup>T. Anderson, *Plasma Antennas* (Artech House, 2011).
- <sup>3</sup>G. G. Borg, J. H. Harris, D. G. Miljak, and N. M. Martin, *Appl. Phys. Lett.* **74**, 3272 (1999).
- <sup>4</sup>J. P. Rayner, A. P. Whichello, and A. D. Cheetham, *IEEE Trans. Plasma Sci.* **32**, 269 (2004).
- <sup>5</sup>I. Alexeff, T. Anderson, S. Parameswaran, E. P. Pradeep, J. Hulloli, and P. Hulloli, *IEEE Trans. Plasma Sci.* **34**, 166 (2006).
- <sup>6</sup>M. Chateaufneuf, J. Dubois, S. Payeur, and J.-C. Kieffer, *Appl. Phys. Lett.* **92**, 091104 (2008).
- <sup>7</sup>M. Alshershby, Z. Hao, and J. Lin, *Phys. Plasmas* **19**, 123504 (2012).
- <sup>8</sup>Y. Ren, M. Alshershby, J. Qin, Z. Hao, and J. Lin, *J. Appl. Phys.* **113**, 094904 (2013).
- <sup>9</sup>Y. Ren, M. Alshershby, Z. Hao, Z. Zhao, and J. Lin, *Phys. Rev. E* **88**, 013104 (2013).
- <sup>10</sup>B. Prade, A. Houard, J. Larour, M. Pellet, and A. Mysyrowicz, *Appl. Phys. B* **123**, 40 (2017).
- <sup>11</sup>P. Polynkin and M. Kolesik, *Phys. Rev. A* **87**, 053829 (2013).
- <sup>12</sup>A. Couairon and A. Mysyrowicz, *Phys. Rep.* **441**, 47 (2007).
- <sup>13</sup>S. L. Chin, S. A. Hosseini, W. Liu, Q. Luo, F. Théberge, N. Aközbeke, A. Becker, V. P. Kandidov, O. G. Kosareva, and H. Schröder, *Can. J. Phys.* **83**, 863 (2005).
- <sup>14</sup>J. Kasparian and J.-P. Wolf, *Opt. Express* **16**, 466 (2008).
- <sup>15</sup>T.-J. Wang, Y. Wei, Y. Liu, N. Chen, Y. Liu, J. Ju, H. Sun, C. Wang, H. Lu, J. Liu, S. L. Chin, R. Li, and Z. Xu, *Sci. Rep.* **5**, 18681 (2015).
- <sup>16</sup>L. Arantchouk, B. Honnorat, E. Thouin, G. Point, A. Mysyrowicz, and A. Houard, *Appl. Phys. Lett.* **108**, 173501 (2016).
- <sup>17</sup>Y. Brelet, A. Houard, G. Point, B. Prade, L. Arantchouk, J. Carbonnel, Y.-B. André, M. Pellet, and A. Mysyrowicz, *Appl. Phys. Lett.* **101**, 264106 (2012).
- <sup>18</sup>F. Théberge, J.-F. Daigle, J.-C. Kieffer, F. Vidal, and M. Châteaufneuf, *Sci. Rep.* **7**, 40063 (2017).
- <sup>19</sup>M. Chateaufneuf and J. Dubois, *SPIE Newsroom* **10**, 0506 (2006).
- <sup>20</sup>W. Liu, F. Théberge, E. Arévalo, J. F. Gravel, A. Becker, and S. L. Chin, *Opt. Lett.* **30**, 2602 (2005).
- <sup>21</sup>Z. Hao, J. Zhang, X. Lu, T. Xi, Z. Zhang, and Z. Wang, *J. Opt. Soc. Am. B* **26**, 499 (2009).
- <sup>22</sup>T. D. Walker and H. J. Christian, *Novel Observations in Lightning Spectroscopy* (Norman, 2014).
- <sup>23</sup>P. Castera and P. Q. Elias, *IEEE Trans. Plasma Sci.* **42**, 1922 (2014).
- <sup>24</sup>W. Li, G. Wang, D. Xiang, and X. Su, *Phys. Plasmas* **23**, 113302 (2016).
- <sup>25</sup>M. M. Abbasi and S. Asadi, *Microwave Opt. Technol. Lett.* **59**, 806 (2017).
- <sup>26</sup>F. Théberge, W. Liu, P. Tr. Simard, A. Becker, and S. L. Chin, *Phys. Rev. E* **74**, 036406 (2006).
- <sup>27</sup>Y. E. Geints and A. A. Zemlyanov, *J. Opt. Soc. Am. B* **31**(4), 788 (2014).
- <sup>28</sup>A. V. Mitrofanov, A. A. Voronin, D. A. Sidorov-Biryukov, A. Pugžlys, E. A. Stepanov, G. Andriukaitis, T. Flöry, S. Ališauskas, A. B. Fedotov, A. Baltuška, and A. M. Zheltikov, *Sci. Rep.* **5**, 8368 (2015).
- <sup>29</sup>P. Panagiotopoulos, P. Whalen, M. Kolesik, and J. V. Moloney, *Nat. Photonics* **9**, 543 (2015).